Aluminothermic synthesis of refractory high entropy alloy Al-Cr-Mo-Ti-V

Carolin Maier, Prof. Dr. Ing. Dr.h.c. Bernd Friedrich

IME Process Metallurgy and Metal Recycling, Institute of RWTH Aachen University
Intzestraße 3
52056 Aachen, Germany

Keywords: Refractory high entropy alloy, RHEA, aluminothermic reduction, pyrometallurgy

Abstract

High entropy alloys (HEAs) are an emerging young alloy group with growing attention in recent years. Especially, HEA including refractory metals (RHEAs) with outstanding properties even at high temperatures show great potential to meet the rising requirements in special applications like in aerospace or nuclear industry. In detail particular suitability is given in use as high-temperature load-bearing structures, thermal insulations and heat exchanger parts.

There is a wide range of production methods for HEA, typical examples are vacuum arc melting, vacuum induction melting or high energy ball milling. All these processes share the same challenges as they typically require both expensive highly purified feed materials and special processing techniques with high energy consumption. In contrast, metallothermic reduction processes enable to improve current production possibilities regarding cost- and time-saving. To understand reaction mechanisms behind the complex system of RHEA a stepwise production of ternary, quaternary and quinary alloys consisting of the elements Al, Cr, Mo, Ti and V will be examined. For proof of principle, objectives are to determine whether an alloy composition can be reached near its target composition or the calculated composition modelled using FactSage software, which problems may occur by increasing the number of oxides and how do the metal oxides interact with each other. The final products, alloy and slag, will be characterized by using inductively coupled plasma atomic emission spectroscopy (ICP-OES), X-ray fluorescence (XRF) and X-ray diffraction (XRD).

First experiments were carried out with feed material, which was stoichiometrically assembled to the expected alloy in case of complete conversion. The alloy obtained showed difficulties with oxygen-affine elements like Ti and Al. For this reason, further research is planned to prove various ways to produce RHEAs. There are several possibilities like separate production of master alloys for subsequent remelting step or utilization of fluxes in aluminothermic reduction for better conversion of the metal oxides to generate finally aimed RHEAs.

Introduction

Nowadays, metals in their pure form are rarely used; there are only few examples like in optical or electrical cables. The reason for that is the increased usage of alloys that are utilized for special and everyday applications due to their improved mechanical, physical and chemical properties. There are currently 30 well researched alloy systems serving a practical purpose. The most important representatives are high-speed steel for tools, stainless steel, superalloys for high-temperature applications, aluminum alloys with high specific strength, and many others that have become indispensable in everyday life. These alloys are mostly multicomponent alloys, or multi-principal element alloys; they all have in common to consist of one main element, to which small quantities of alloying elements are usually added. [1, 2] Figure 1 shows the areas in ternary and quaternary alloying systems which are well known in phase diagrams (grey areas), while the white ones are mostly still unexplored [3].

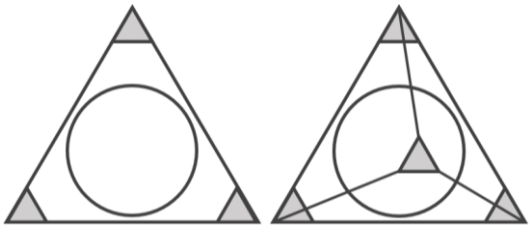

Figure 1: Schematic illustration of a ternary and quaternary alloying system, adapted from [3]

The reason for the low attraction of research in this area can be explained by the results of Archard at the beginning of the 19th century. He mixed five to seven alloying components with equal masses and produced the first HEAs. Properties of obtained alloys were various, but not beneficial. [4] Furthermore, these new alloys have enormous amounts of data to be collected, analyzed and evaluated. The effort for a seven-component phase diagram would cost as much effort and time as the establishment of 4000 binary and 8000 ternary phase diagrams in the last 100 years. [5, 6] Nevertheless, at the beginning of the millennium research grew on this topic, with a resulting new alloy type called HEA.

Although today's alloys already show a good combination of properties, there is always a need for further optimization in high-tech applications. In the optimum case, alloys present a great match with the properties listed below [7]:

- Strength and toughness: high stiffness, strength and toughness
- Wear resistance: high resistance to wear and high hardness
- Environmental resistance: high resistance to (stress) corrosion
- Weight: light weight, low density
- Formability: superplasticity and high elongation rate
- Magnetism: good soft or hard magnetic properties
- Green materials: environmentally friendly, recyclable, lead and cadmium free

The new alloy group of HEAs shows considerable potential for achieving these improvements.

There are two basic definitions of HEAs: The first definition refers to the composition. According to this, HEAs are precisely those alloys that contain at least five and at most 13 major elements, with each major element contributing between 5 and 35 at.-% to the alloy. A minor element is defined as any added element contributing less than 5 at.-%. [7, 8] The second definition is based on the so-called high entropy effect. Thermodynamically, a system will try to minimize its Gibbs energy at a given temperature and constant pressure [9, 10]. Gibbs energy is defined as enthalpy minus entropy multiplied by temperature. When the Gibbs energy is considered before and after mixing, it is referred to as the Gibbs energy of mixing, in which mixing enthalpy and mixing entropy are part of the equation. Since the mixing entropy results primarily from the configuration entropy, it can be simplified. By definition, the mixing entropy (and so the configuration entropy) increases with an increase in the number of metals contained in the alloy; that results in the high entropy effect. A detailed overview of the derivation can be taken from Yeh's [9, 10, 11] publications. The derivation results in equation (1) for HEAs.

$$\Delta S_{config} \geq 1.5 \cdot R \quad (1)$$

ΔS_{config}: configuration entropy [$J \cdot K^{-1}$]; R: general gas constant [$J \cdot K^{-1} \cdot mol^{-1}$]

For commercial alloys, the configurational entropy is below 1.5 · R due to containing fewer elements. For example, high-speed steel M2 has 0.73 · R and aluminium alloy 2024 only 0.29 · R. [11]

Both definitions presented should not be considered as strict rules, but rather as guidelines for the classification of the alloy group HEA. So, the most important aspect of the HEA concept is that the high entropy of mixing ensures the formation of a random solid solution and inhibits the creation of an ordered phase. [4, 8, 12]

There is a wide range of possible synthesis routes for HEAs. Figure 2 presents the most important manufacturing routes. [12, 13] Depending on the particular application of the HEA, different manufacturing methods are preferred. For example, physical vapor deposition is more commonly used to produce thin-layered surfaces, whereas mechanical alloying is preferred for powder production. [12] In literature, vacuum arc melting is mostly presented as manufacturing process for HEAs [8, 13].

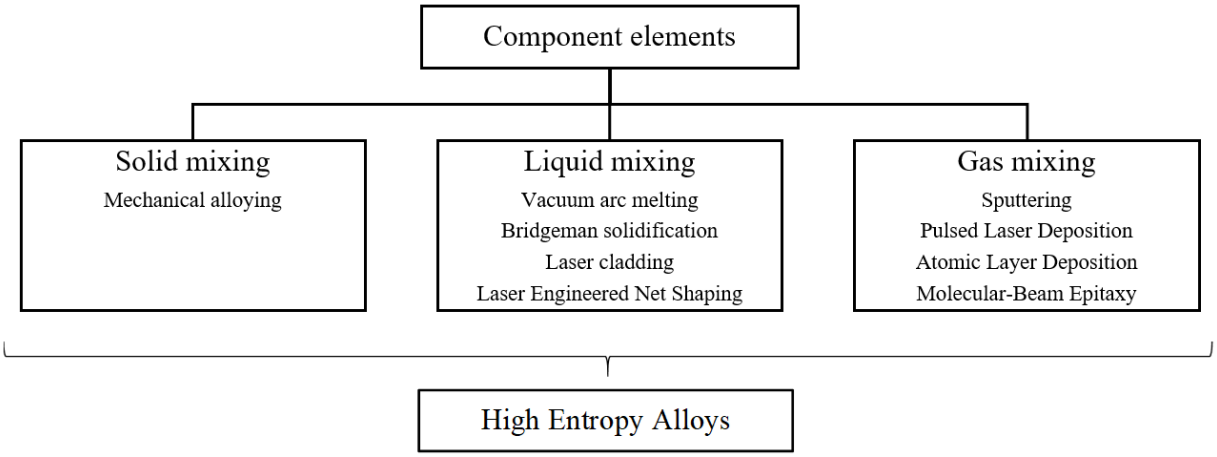

Figure 2: Various production routes for synthesis of HEA, adapted from [4]

This is preferable above all for the production of small quantities of alloys; however, the production of alloys on an industrial scale is hardly feasible with this method. All synthesis routes have in common that they require high energy consumption, use of pure metals as input material and at the same time have to be carried out under vacuum/inert atmosphere to prevent atmospheric contamination. Simultaneously, only small-scale production has been investigated so far.

Fundamentals on metallothermic reduction

Metallothermy is generally defined as pyrometallurgical reduction of metal compounds, as oxides, chlorides or fluorides, by a less noble metal or metal compound. From the technical and economic point of view, the use of sodium, potassium, magnesium, calcium, silicon, and aluminum as reduction metals is common nowadays. [14] The general reaction equation of a metallothermic reaction can be represented by the following formula [14, 15]:

$$a \cdot MeX + b \cdot R \rightarrow c \cdot Me + d \cdot RX \quad (2)$$

Me: metal; X: chlorine, fluorine or oxygen; R: reduction agent;

a, b, c, d: stoichiometric coefficient

A quantitative measure for the stability of metal compounds is the free reaction enthalpy, which is given by the equations (3) and (4).

$$\Delta G° = \Delta H° - T \cdot \Delta S° \quad (3)$$

and

$$\Delta G° = - R \cdot T \cdot \ln(K) \quad (4)$$

For pure substances, in this case oxides, the standard free enthalpy of reaction can be simplified according to equation (5) to the so-called oxygen potential.

$$\Delta G° = - R \cdot T \cdot \ln(K) = - R \cdot T \cdot \ln((a_{MeO}) \cdot (a_{Me} \cdot p_{O2})^{-1}) = R \cdot T \cdot \ln (p_{O2}) \quad (5)$$

R: gas constant (8.314 $J \cdot mol^{-1} \cdot K^{-1}$); T: temperature (K); k: equilibrium constant;
a_{MeO}: activity of metal oxide; a_{Me}: activity of metal; p_{O2}: oxygen partial pressure

The reaction can only proceed spontaneously if a negative enthalpy of reaction ΔG is present. The Richardson-Jeffes diagram (see Figure 3) shows whether a particular metal oxide will be reduced by a chosen reduction metal at a certain temperature. The diagram illustrates the Gibbs energy released by oxidation of a selected metal as a function of temperature. Reduction is possible when the free enthalpy of oxide formation of the resulting metal compound (RX) is more negative than that of the input metal compound (MeX). [14] Furthermore, the larger the difference between the two free enthalpies of formation, the higher the driving force of the metallothermic reduction. With increasing temperature, the reduction of all metal compounds is energetically more favorable, since these are more unstable from a thermochemical point of view; this applies to oxides as well as to chlorides and fluorides. [15]

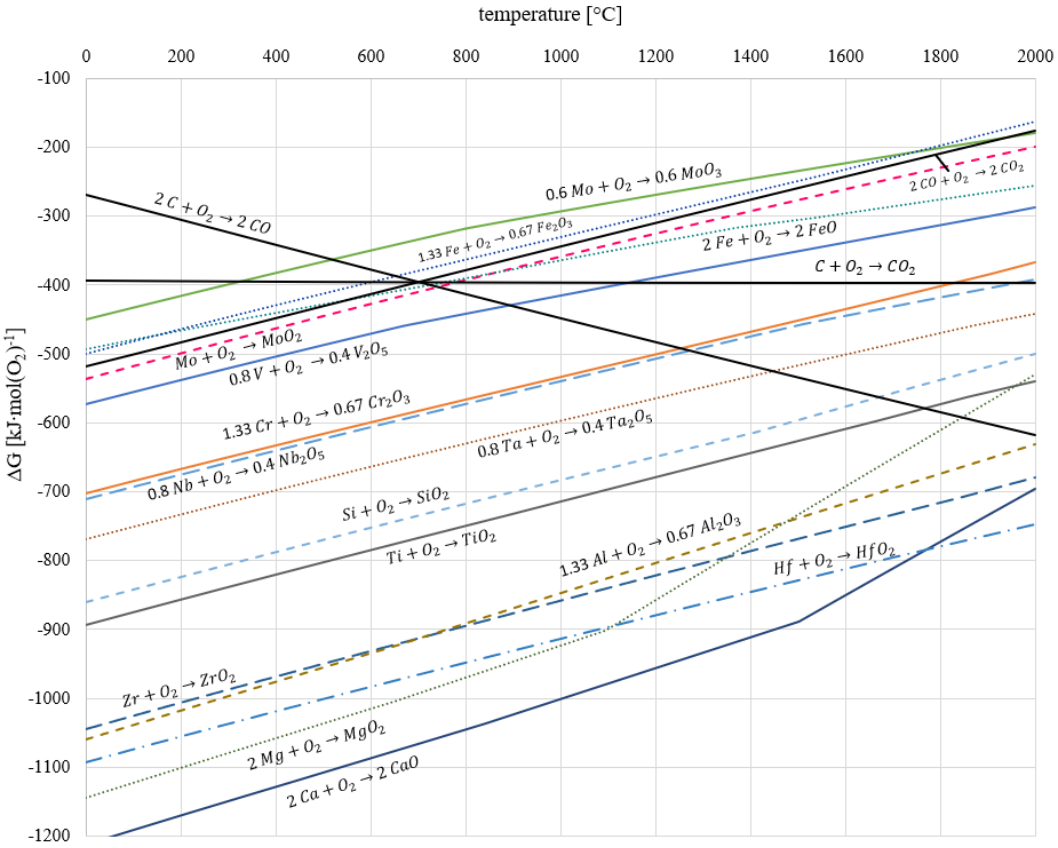

Figure 3: Richardson-Jeffes Diagram for pure metals [16]

However, the diagram shown in Figure 3 has some limitations as it does not include the kinetics of the reaction. Especially at low temperatures the reaction rate can be so small that a predicted reaction does not take place. [17] Furthermore, activities are neglected. For substances in solution, the activity can be calculated using equation (6).

$$a_i = \gamma_i \cdot X_i \qquad (6)$$

a_i: activity of component i; γ_i: activity coefficient of component i;

X_i: mole fraction of component i

The activity coefficient provides information about the deviation from an ideal solution. In the case of metal/slag equilibria, the activity of the oxides to be reduced in the metal and slag phase is of particular importance, since the activity is influenced by the temperature and the composition. Thus, for a reduction of oxides, a higher activity in the slag is advantageous, and for slagging, a low activity in the slag is correspondingly advantageous. [18]

Based on the known reaction enthalpies and empirical values, Shemtchushny has established a rule (SH factor) for the self-sustaining nature of metallothermic reactions. According to Shemtchushny, the amount of heat released, also called specific heat effect, for a self-sustaining production of ferroalloys must be 2300 $J \cdot g^{-1}$ input quantity. Dautzenberg generalized this value for metallothermic reductions to 2700 $J \cdot g^{-1}$. [15]

The specific heat effect can be calculated by formula (7) [15]:

$$SH = \frac{\Delta H_R}{\sum m(\text{input material})} \quad (7)$$

SH: Shemtchushny factor [$J \cdot g^{-1}$], ΔH_R: standard enthalpy of reaction [J]

The rules presented should only be used as indication. Studies showed that the optimal energy density depends primarily on the desired alloy system. For the thermite reaction, for example, an energy density of 2980 $J \cdot g^{-1}$ is necessary, while the W-Al system only require an energy density of 1900 $J \cdot g^{-1}$ [19].

Experimental

In this publication, the possibility of obtaining the RHEA Al-Cr-Mo-Ti-V aluminothermically is evaluated. This alloy is described for the first time in a paper by Udoeva et al. [20] in which the aluminothermic reduction was modelled by HSC Chemistry. The production of RHEAs metallothermically has some advantages; for example, refractory alloys show high liquidus temperatures which are difficult to achieve by common melting processes. Furthermore, input material of the refractory alloys are oxides which are less expensive than the metals in desired purity. By simultaneous aluminothermic conversion of the refractory metal oxides, alloys can be directly produced without further synthesis in an additional process.

At the same time, it can be exploited that the reductions of different refractory metal oxides release various quantities of thermal energy. Table 1 shows specific reaction enthalpies and corresponding SH factors of relevant metal oxide reductions in experimental procedure. During reduction of TiO_2, lower energy in form of heat is released compared to reductions of other refractory metal oxides. The co-reduction of various refractory metal oxides lead to the support of the non-autothermal reduction of TiO_2, so that the overall reaction becomes autothermal.

Table 1: Reaction enthalpies and SH factors for selected aluminothermic reductions calculated with FactSage [16]

	Reaction enthalpy ΔH_R [kJ]	**SH factor [$J \cdot g^{-1}$]**
$0.5\ Cr_2O_3 + Al \rightarrow Cr + 0.5\ Al_2O_3$	-274.29	-2663.6
$0.75\ MoO_2 + Al \rightarrow 0.75\ Mo + 0.5\ Al_2O_3$	-396.96	-3229.0
$0.75\ TiO_2 + Al \rightarrow 0.75\ Ti + 0.5\ Al_2O_3$	-129.29	-1488.1
$0.3\ V_2O_5 + Al \rightarrow 0.6\ V + 0.5\ Al_2O_3$	-372.67	-4570.1

In this paper, the main focus is on the production of HEAs with nearly equal mass fractions by aluminothermic reduction. For this purpose, an experimental plan was prepared which shows the desired compositions for various alloying systems (see Table 2).

Table 2: Experimental plan for the production of different alloys of RHEA Al-Cr-Mo-Ti-V

Alloy	**Composition [wt.-%]**				
	Al	Cr	Mo	Ti	V
Al-Cr-Ti	33.33	33.33	0	33.33	0
Al-Ti-V	33.33	0	0	33.33	33.33
Al-Cr-V	33.33	33.33	0	0	33.33
Al-Cr-Ti-V	25	25	0	25	25
Al-Cr-Mo-Ti-V	20	20	20	20	20

Initially, five test series (two trials each) are conducted; three ternary systems Al-Cr-Ti, Al-Cr-V and Al-Ti-V, one quaternary system Al-Cr-Ti-V and one quinary system Al-Cr-Mo-Ti-V are produced. For economic reason, MoO_2 is only used in the last trial. Target alloy mass is 7500 g; adjusted alloy systems have a target amount of 5500 g. The input material masses can be seen in Table 3; a stoichiometric conversion is assumed. As fluxing agent, lime (CaO) has been added. An Al_2O_3/CaO ratio of 70/30 wt.-% was selected to lower the liquidus temperature and viscosity of slag to improve the metal/slag separation. The selected SH factor is 2500 $J \cdot g^{-1}$; if the system is below the target SH factor, potassium perchlorate ($KClO_4$) is used as booster. For systems with higher SH factor without booster addition, the test is provided with the SH factor achieved. Adjustments of energy density only take place when conversion is insufficient.

Table 3: Input material mixture with adiabatic temperature and SH factor for each trial [16]

Alloy	**Input material [g]**							**Ad. T [°C]**	**SH [J·g^{-1}]**
	Al	Cr_2O_3	MoO_2	TiO_2	V_2O_5	$KClO_4$	CaO		
Al-Cr-Ti	6436	3617	0	4130	0	1573	3208	2086.3	-2800
Al-Ti-V	6710	3617	0	4130	0	2102	3430	2056.1	-2500
Al-Cr-V	6830	0	0	4130	4418	598	3527	2270.6	-2580
Al-Cr-Ti-V	5948	3617	0	0	4418	0	2812	2090.6	-2600
Al-Cr-Ti-V (adj.*)	6301	3558	0	4259	4402	748	3584	2126.1	-2500
Al-Cr-Mo-Ti-V (adj.*)	5583	3123	2849	3909	3916	560	3306	2168.2	-2600

***adj.: The input material mix of these trials were adjusted after first analysis through XRF**

As shown in Figure 4, experiments are conducted in alumina lined steel reactors (500 x 500 x 500 mm) with a filling capacity of approx. 25 L (Ø 300 mm, 400 mm height). The reactors are placed under an integrated suction system to prevent dust and excessive exhaust emission. The material is weighed, placed in a drum and homogenized in a drum-hoop mixer for 30 minutes. The input mixture is then filled into the alumina lined reactors; it is electrically ignited through an

ignition pack containing the ignition mixture $KClO_4$ (40 wt.-%), Mg chips (10 wt.-%) and Al granules (50 wt-%). XRF (Bruker CTX 800) and ICP-OES (Spectro CIROS Vision) are used for compositional analysis; XRD powder spectrometer with a copper anode (40 kV, 30 mA) is further used for structural analysis.

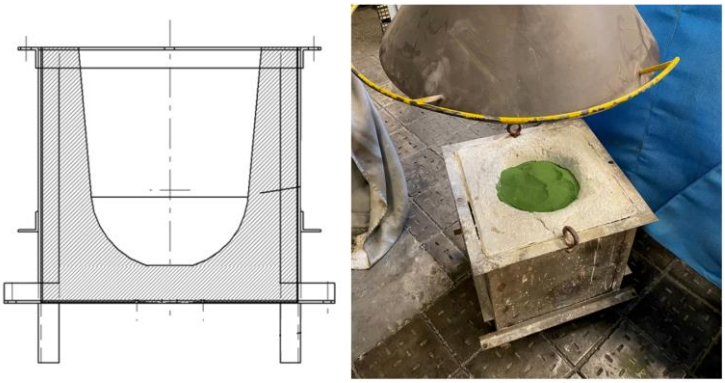

Figure 4: Technical drawing of reactor with alumina lining and actual setup for experiments conducted

In advance, thermochemical studies are carried out on the considered HEA system to investigate the extent to which stoichiometric conversion works from a thermochemical point of view for this specific alloy system. Therefore, thermochemical modelling was done with FactSage 7.3 using following databases: FactPS, FToxid and SGTE [16].

Results

Twelve trials were carried out in total investigating five different alloy systems, two trials per alloy system. Each trial indicated a conversion of the input material and both metal and slag phase were formed. Metal samples were first analyzed using XRF; later all samples (metal and slag) were examined with ICP-OES. After conducting the experiments on the ternary and quaternary alloy systems, first metal samples were analyzed using XRF and the results evaluated. For further investigation, the subsequent trials (quaternary and quinary alloy system) were corrected by suitable adjustments (see equation (9) and (10)). The adjusted trials are marked by "(adj.)".

Following parameters were recorded during trials conducted: reaction time, metal mass and slag mass. The parameter reaction time was difficult to define because of subjective view on the process. Videos were made during the trials and used to define the reaction time. The beginning of the reaction starts with the ignition, which can be determined very precisely. In the following some points are mentioned, which define the termination of the reaction: strong smoke emission subsides, no visible movement of the slag surface, no slag splashing out of the reactor.

Metal yields could be derived by recording the metal and slag masses. The metal yield in the experiments is the actual amount of alloy generated in relation to the expected amount of alloy. The metal yield is calculated by equation (8).

$$\eta_{alloy} = \frac{m_{alloy\ generated}}{m_{alloy\ target}} \quad (8)$$

η_{alloy}: metal yield; $m_{alloy\ generated}$: generated alloy mass [g]; $m_{alloy\ target}$: target alloy mass [g]

Conversion rates of metals in the alloy were calculated based on the resulting metal masses and the contents analyzed by ICP-OES, as stated in equation (9). Assuming stoichiometric conversion for each metal oxide, the expected metal quantity is the corresponding quantity in the alloy. For Al the conversion rate is calculated different: Al is both reducing agent and alloying component. Thus, Al must be added over-stoichiometrically to achieve the target alloy composition. For Al, the expected metal mass in the alloy is the amount, which comes additionally into the input system besides the amount which is added to perform the reduction. This means that the conversion rate of Al can be higher than 100 % because insufficient reduction of metal oxides in the input system leads to an excess of Al in the alloy. For the other metals this effect can be excluded (exception within the adjusted trials).

$$\eta_{Me,alloy} = \frac{m_{alloy} \cdot c_{Me,alloy}}{m_{Me,expected}} \quad (9)$$

The adjustment of initial mixture was based on the conversion rates determined by XRF analysis. Assuming the complete, stoichiometric conversion, a conversion rate for each metal oxide in the initial mixture was determined. Based on this conversion rate, the addition amounts of the corresponding metal oxides were adjusted, as shown in equation (10).

$$m_{MeO,adjusted} = \frac{m_{MeO,stoichiometric}}{\eta_{Me,alloy}} \quad (10)$$

$\eta_{Me,alloy}$: conversion rate for Me in alloy; m_{alloy}: alloy mass [g]; $c_{Me,alloy}$: conc. of Me in alloy (ICP-OES/XRF); $m_{Me,expected}$: expected mass of Me in alloy [g]; $m_{MeO,adjusted}$: adjusted mass of MeO in initial mixture [g]; $m_{MeO,stoichiometric}$: stoichiometric mass of MeO in initial mixture [g]

Alloy system Al-Cr-Ti

Aluminothermic reduction trials for generation of Al-Cr-Ti alloy required higher reaction times than the trials on the other alloy systems (in average 286 s instead of 128 s). In addition to typical slag and metal phases, an undesirable top layer of unreacted material, as shown in Figure 5, remained resulting in losses in metal yield. Both, slag and metal phase, have a high hardness; the metal ingot is not brittle, so it can only be removed as a whole ingot. This caused the problem that not all alloys could be analyzed because the analytical equipment could not handle the dimensions of the ingot. Crushing was not possible due to the high hardness, as sawing was only possible to a limited extent.

As shown in Figure 9, the desired alloy composition could not be reached. The Al content is higher than expected, both TiO_2 and Cr_2O_3 were not sufficiently reduced. This leads to the assumption, that

reduction of TiO_2 and Cr_2O_3 did not take place adequately what also can be caused by the presence of unreacted material on the top layer.

In slag analysis, high amounts of Ti are detected (12.5 wt.-% and 6.4 wt.-%). This results in too low values for Al- and Ca-oxide in slag phase. The relative ratio of Al_2O_3/CaO is 76.70 wt.-% to 23.3 wt.-% for trial 1 and 69.32 wt.-% to 30.68 wt.-% for trial 2, which corresponds approximately to the desired slag composition.

Figure 5: Unreacted top layer and metal ingot of trial Al-Cr-Ti

Alloy system Al-Ti-V

The resulting slag shows a smooth surface in yellowish color (see Figure 6). The metal is brittle and can easily be divided into small pieces.

In trial 2 a high metal yield of 97.7 % could be obtained. Ti exhibits higher conversion rates in this alloy than in the Al-Cr-Ti system (in average 73.5 % instead of 65.6 %). The reduction of V_2O_5 worked efficiently. In trial 1, a conversion rate of 92.3 % was detected; in trial 2, however, 113.5 % have been achieved. For this reason, a measurement error in trial 2 is expected; nonetheless, for the second trial high conversion rate for V_2O_5 reduction is assumed.

Figure 6: Slag surface and metal of trial Al-Ti-V

As illustrated in Figure 9, Ti-oxide concentration in the slag are also comparably high as in the reduction trials on the Al-Cr-Ti system (8.8 wt.-% and 11.8 wt.-%). So, the average Ti content is a little higher than in the system Al-Cr-Ti.

Alloy system Al-Cr-V

In this system, the energy densities of the oxide reduction of Cr_2O_3 or V_2O_5 are sufficiently high so that the reaction does not require any addition of booster. There was no significant spattering of slag observed and smoke generation was moderate. The reaction proceeds calmly and below the powdery surface of input material. The resulting metal is brittle and metal yields are both above 90 %. The slag shows a green-brownish color and a smooth surface, as illustrated in Figure 7.

In the Al-Cr-V alloy system, aimed composition of 33.3 wt.-% of Al, Cr and V has been almost achieved in both trials. Hence, this test series is the most successful by reaching desired composition within a range of ± 1 wt.-%. As illustrated in Figure 11, the conversion rates are high, exceeding 90 % for each metal contained in the alloy.

Contamination of the slag by Cr_2O_3 or V_2O_5 are low; nevertheless, Al_2O_3 content of the slag is lower than expected (53.3 wt.-% and 60.1 wt.-%). Against the background of only slightly deviating alloy composition, low Al_2O_3 concentration in slag is obviously contrary to the expectation and cannot be explained sufficiently.

Figure 7: Slag surface and metal of trial Al-Cr-V

Alloy system Al-Cr-Ti-V

Aluminothermic reduction experiments show relatively high reaction times of 170 s and 190 s (see Figure 8). At the same time, strong smoke formation is observed as well as slag splashing out of the reactor during the trials. Resulting products are a slag with smooth brownish surface and a brittle metal phase. The metal yields of 92.7 % and 93.7 % are in a very good range.

The metal composition does not reach the intended specification. The resulting alloy has too high Al content, whereas TiO_2 is reduced much worse. The conversion rates for TiO_2 range from 72.8 % to 79.3 %. Cr_2O_3 and V_2O_5 react better in this system, but it can be seen that V_2O_5 is reduced to a greater extend compared to Cr_2O_3, resulting in higher conversion rates.

In the slag phase, Ti-oxide content is relatively low compared with the ternary alloy systems containing Ti (see Figure 9: 8.1 wt.-% and 5.9 wt.-%). The other two components of the feed mixture, Cr and V, both show an impurity level below 0.6 wt.-%.

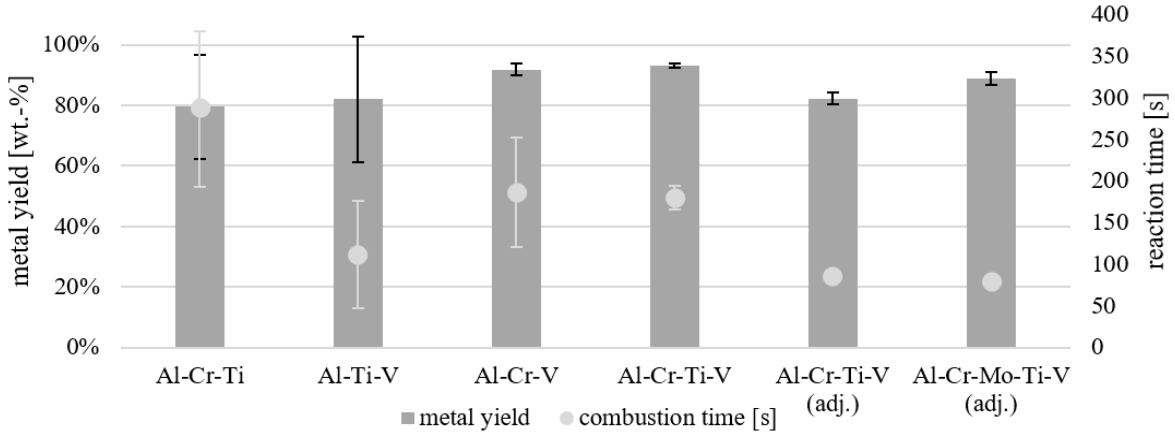

Figure 8: Average of metal yield and reaction time (with standard deviation) for reduction trials listed in Table 3

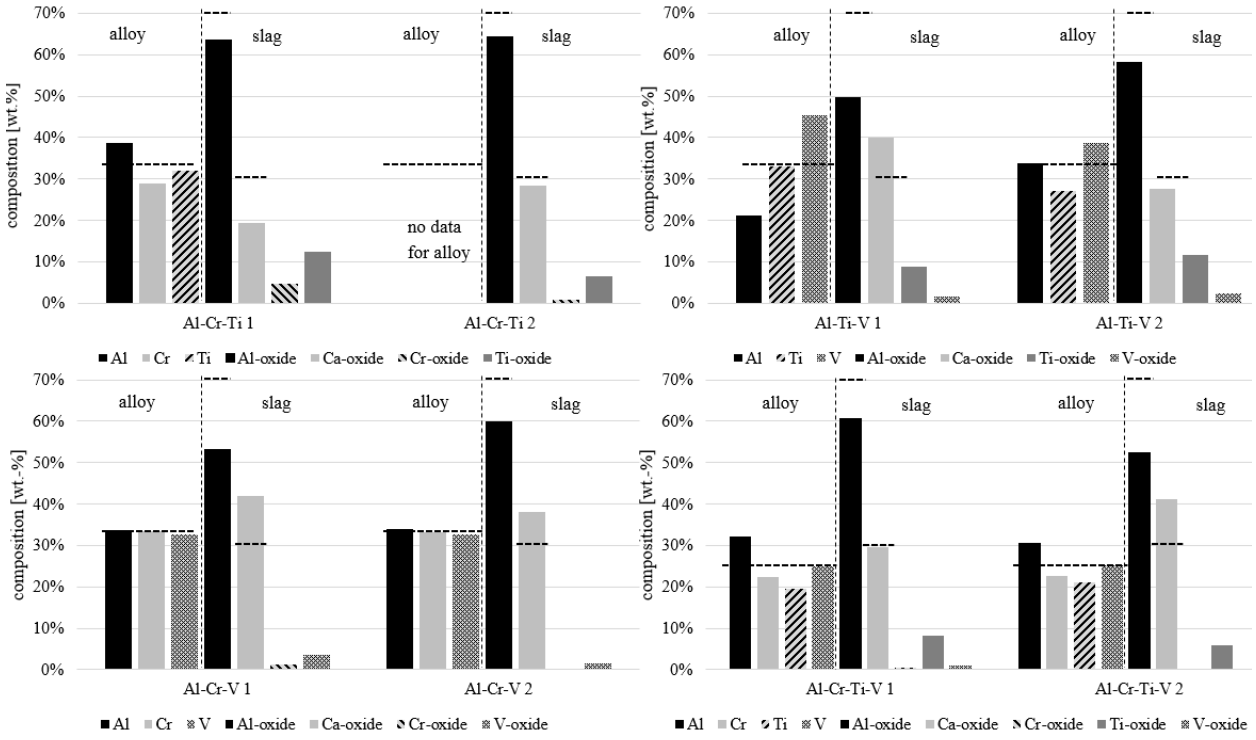

Figure 9: Composition of metal and slag produced in the reduction trials listed in Table 3 (ternary and quaternary trials)

Alloy system Al-Cr-Ti-V (adj.)

The first adjusted trial show significantly lower reaction time compared to tests without adjustment (80 s and 90 s). At the same time, the metal yield drops to 80.8 % and 83.6 %. In comparison to the alloy system Al-Cr-Ti-V without adjustment, the experiments are turbulent. There is strong splashing of slag and the formation of smoke rises. The slags are dark brown in color and show an even surface (see Figure 10). The metal is brittle.

Figure 10: Slag surface and metal of trial Al-Cr-Ti-V (adj.)

The Ti content is almost unchanged although the addition of TiO_2 to the input system is over-stoichiometric. The conversion rates of TiO_2 drop to about 60 % in both trials. For Cr_2O_3 and V_2O_5, on the other hand, over-stoichiometric addition can be clearly seen in the alloy composition as pictured in Figure 13. For Cr, the concentrations increase to 27.6 wt.-%. and 29.9 wt.-%, for V to 32.7 wt.-% and 30.9 wt.-% instead of the targeted 25 wt.-%. Only for Al content it can be observed that significantly less is present in the alloy. This is due to the increased reduction of Cr_2O_3 and V_2O_5.

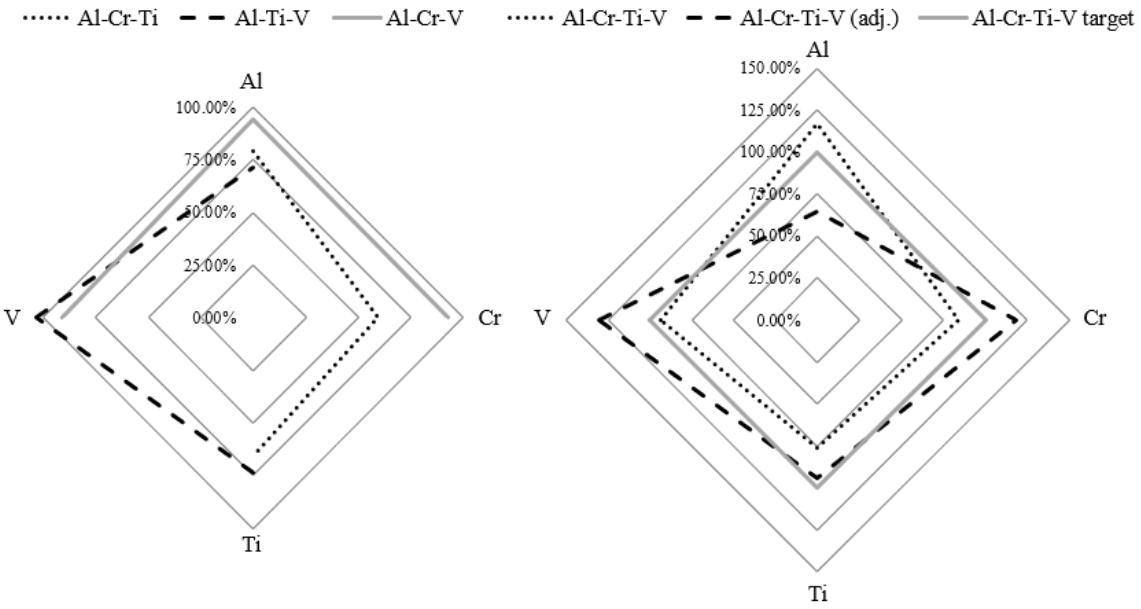

Figure 11: Conversion rates of ternary and quaternary alloy systems obtained

The slag shows a similar composition for the stoichiometric and over-stoichiometric input systems. The Ti-oxide content in the slag increases to 10 to 12 wt.-%. The relative ratio between Al_2O_3 and CaO remains constant.

Alloy system Al-Cr-Mo-Ti-V (adj.)

Both trials on the five-substance system show very similar results and thus little deviation. The time for reduction is comparable to the Al-Cr-Ti-V (adj.) system.

The target equimass 20 wt.-% for each metal in the alloy is not achieved. Cr (24.8 wt.-% and 24.7 wt.-%), Mo (27.7 wt.-% and 27.8 wt.-%) and V (both 26.4 wt.-%) react over-stoichiometrically in this system whereas Al and Ti show a lower proportion in the alloy. The contents are far off the targeted content at 10.7 wt.-% and 10.7 wt.-% for Ti, 9.2 wt.-% and 9.3 wt.% for Al. The conversion rates of Ti in these reactions are below 50 %.

Nevertheless, the expected phases could be determined in the XRD analysis (see Figure 12). Qualitatively, the phases Cr0.333 Mo0.333 V0.334 and AlTi could be detected, which indicates that the desired phases have occurred and can be determined.

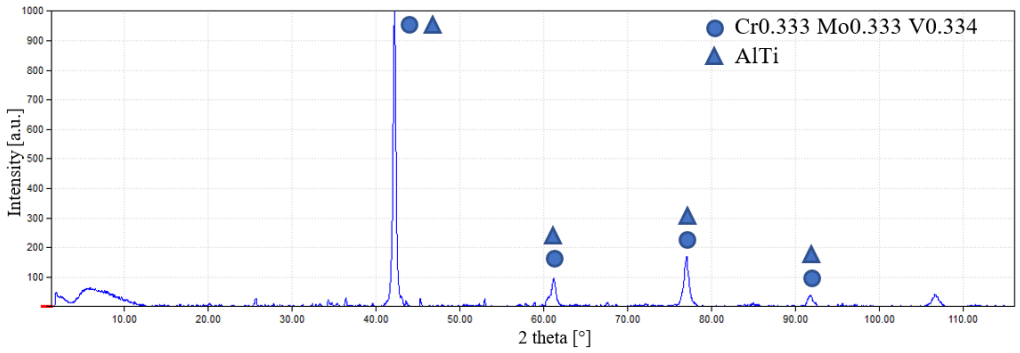

2 theta	Peak height
6.28	62.2
6.42	60.4
6.57	61.7
7.37	57.3
42.24	1000
61.22	96.4
61.41	65.4
76.81	123.5
77.05	169.4
77.26	105.8

Figure 12: XRD-pattern of metal sample from trial Al-Cr-Mo-Ti-V (adj.) 1

The slag has high levels of Ti-oxide contamination; on average, the slag has a Ti-oxide content of 17.9 wt.-%.

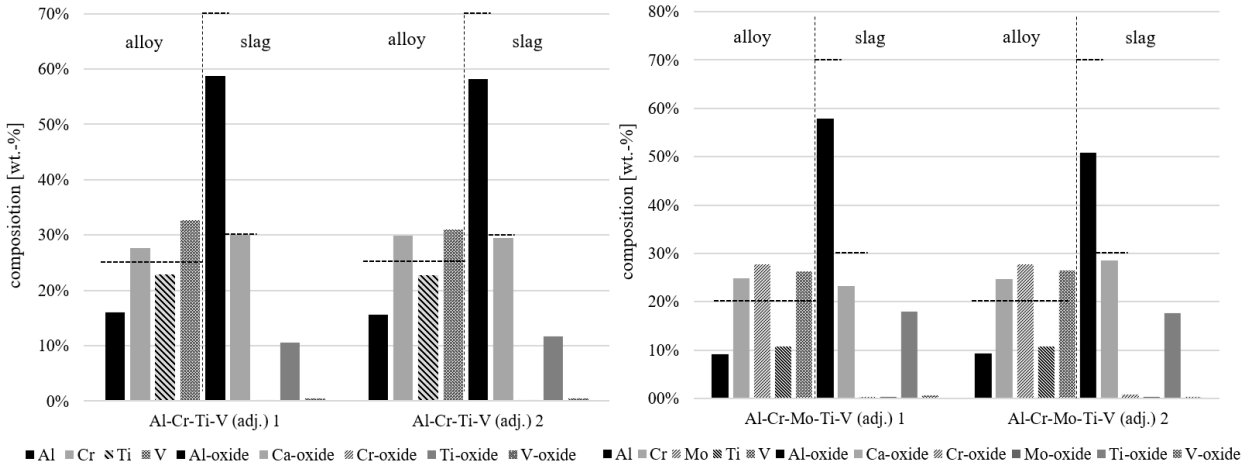

Figure 13: Composition of metal and slag produced in the reduction trials shown in Table 3 (adjusted quaternary and quinary trials)

Comparison to thermochemical calculation through FactSage

From thermochemical point of view, the alloys will mostly not achieve the composition expected. Except for the alloy Al-Cr-V, which achieves the anticipated composition as seen in Figure 14, the other alloys are far behind. It is striking that Ti in particular seems to cause major problems by being largely responsible for the deviation from the targeted composition. This can be justified by the low enthalpy of reaction of TiO_2-reduction (see Table 1 and Figure 3).

Closer examination also reveals that both, Cr_2O_3 and V_2O_5, cause the same effect in their reduction. The Al present for the reduction of the TiO_2 is not consumed in aluminothermic reduction and thus enters the alloy as metallic component. For this reason, higher Al contents are identified in these systems. At the same time, the contents of both Cr and V as alloying constituents are increased in the ternary alloy system Al-Cr-V. This can be attributed to the fact that 100 %-conversion cannot be represented and thus the actual one differs from the targeted alloying amount. For example, in the Al-Cr-Ti system only an alloy mass of 6899 g is achieved instead of the targeted 7500 g assuming stoichiometric conversion.

The unreacted amount of TiO_2, which does not contribute to metal phase in form of Ti, is consequently in the slag. Thus, Ti-oxide contents of up to 12.5 wt.-% are achieved in the ternary systems, and even 19.5 wt.-% in the slag of the quaternary system. Due to the incomplete conversion, the production of the equimass alloy cannot be assumed stoichiometric, especially for the reduction of TiO_2.

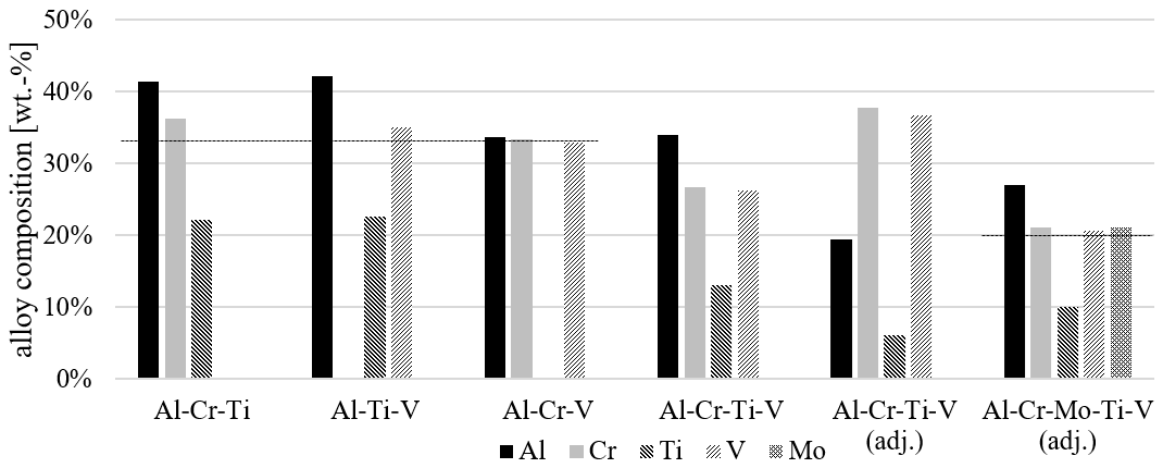

Figure 14: Calculated composition of different alloy systems using FactSage [16]

High Al contents of the alloys predicted by FactSage could also be detected in the trials conducted. This tendency applies to the ternary alloy Al-Cr-Ti (only one alloy analyzable) and the quaternary alloy Al-Cr-Ti-V.

In case of the alloy Al-Cr-Ti, it can be determined that this alloy does not have a higher Cr than Ti content as calculated by FactSage. The alloy obtained in the experiment shows a higher Ti content; this conclusion cannot be confirmed due to absence of analysis of the alloy from trial 2.

As depicted in Figure 15, high contents of Ti-oxide in the slag can also be found in the experimental part. While the contents in unadjusted trials range from 9.4 wt.-% to 10.3 wt.-%, the calculation shows 11.3 wt.-% to 12.5 wt.-% for ternary alloy systems. In the Al-Cr-Ti-V (adj.) and Al-Cr-Ti-Mo-V (adj.) trials, the calculated values do not agree with those in the experimental work. In the calculation, Ti-oxide content is 19.5 wt.-%, whereas in the trials it differs with 11.1 wt.-%. The contrary can be observed for the quinary system. In this case, predicted Ti-oxide concentration is 10.5 wt.-%, while the slag from experimental study shows an average contamination of 17.9 wt.-%.

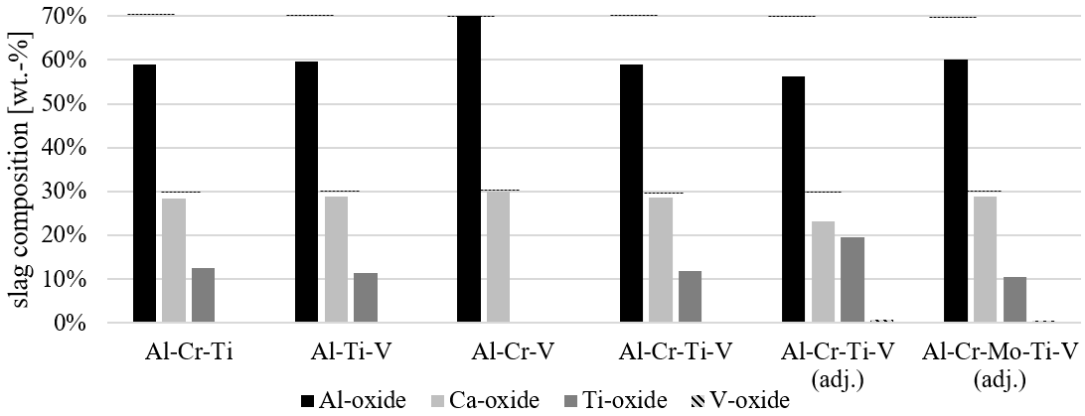

Figure 15: Calculated composition of slag from different alloy systems using FactSage [16]

Conclusion

In this paper the aluminothermic production of RHEAs is investigated exemplified through the alloy Al-Cr-Mo-Ti-V. The main focus is on the chemical composition of alloys obtained and the conversion rates achieved for aluminothermic reduction of various metal oxides. Currently, the production is mainly carried out on laboratory scale. Aluminothermic reduction is considered to be a promising low-cost method for large-scale production of HEAs.

Based on the results, the proof of principle that the synthesis of RHEAs through aluminothermic reduction is possible has been provided. One system shows the possibility of direct production without any adjustment. Al-Cr-V system stands out from the series of experiments on ternary systems. It combines high metal yields with high conversion rates of the individual metal oxides. Moreover, composition targeted is within a range of 1 wt.-%. A low standard deviation suggests constant process control and thus high reproducibility of Al-Cr-V alloy production.

The two ternary systems Al-Cr-Ti and Al-Ti-V cannot achieve similar results. Both show problems in the evaluation because metal yields and conversion rates of metal oxides are far below the expected range. In this experimental series, V shows a better influence on the Ti conversion than Cr. Furthermore, conversion rate of V_2O_5 is higher and at the same time beneficial for Ti-oxide conversion. Thermochemical calculation also confirms this effect: Both metal yield and conversion rates are better for the alloying system containing V (see Table 4 and 6). Hence, the resulting alloy amount of Al-Cr-Ti is about 167 g lower compared to the ternary alloy system Al-Ti-V. Also, shown in Figure 5,

the contamination of slag by Ti-oxides in the thermochemical calculation is lower by using V_2O_5 instead of Cr_2O_3 as an additional oxide in the input mixture (12.50 wt.-% to 11.28 wt.-% Ti-oxide).

Table 4: Average chemical composition of alloys based on ICP-OES results, based on FactSage calculation (cursive) [16] and XRF analysis (bold)

Alloy	Al	Cr	Mo	Ti	V
Al-Cr-Ti	38.59%	28.97%		32.07%	
	41.32%	*36.21%*		*22.09%*	
	55.87%	**23.41%**		**19.73%**	
Al-Ti-V	27.48%			20.10%	42.07%
	42.11%			*22.54%*	*34.97%*
	30.04%			**29.16%**	**39.67%**
Al-Cr-V	33.79%	33.28%			32.67%
	33.59%	*33.40%*			*32.93%*
	57.43%	**21.63%**			**20.16%**
Al-Cr-Ti-V	31.38%	22.55%		20.39%	25.04%
	33.89%	*26.63%*		*12.98%*	*26.20%*
	45.08%	**18.83%**		**17.13%**	**18.38%**
Al-Cr-Ti-V	15.77%	28.77%		22.81%	31.83%
(adj.)	*19.40%*	*37.75%*		*6.08%*	*36.62%*
	13.46%	**31.06%**		**25.35%**	**29.37%**
Al-Cr-Mo-Ti-V	9.24%	24.74%	27.77%	10.68%	26.38%
(adj.)	*12.20%*	*28.34%*	*28.43%*	*3.77%*	*27.15%*
	8.20%	**24.15%**	**33.07%**	**10.49%**	**23.12%**

Table 5: Average chemical composition of slags based on ICP-OES results and based on FactSage calculation (cursive) [16]

Alloy	Al_2O_3	Cr2O3/CrO	MoO_2	TiO_2/Ti_2O_3	$VO/VO_2/V_2O_3$	CaO
Al-Cr-Ti	63.86%	3.42%		9.59%		23.14%
	59.06%	*0.00%*		*12.50%*		*28.35%*
Al-Ti-V	38.64%			10.27%	1.95%	49.16%
	59.57%			*11.28%*	*0.32%*	*28.76%*
Al-Cr-V	56.68%	0.82%			2.50%	40.00%
	70.06%	*0.00%*			*0.00%*	*29.93%*
Al-Cr-Ti-V	56.59%	0.31%		7.02%	0.68%	35.41%
	59.01%	*0.00%*		*11.88%*	*0.34%*	*28.69%*
Al-Cr-Ti-V	58.44%	0.17%		11.12%	0.51%	29.77%
(adj.)	*56.31%*	*0.00%*		*19.54%*	*0.80%*	*23.21%*
Al-Cr-Mo-Ti-V	54.33%	0.52%	0.09%	17.86%	1.33%	25.89%
(adj.)	*60.15%*	*0.00%*	*0.00%*	*10.53%*	*0.40%*	*28.83%*

Table 6: Metal and slag mass based on FactSage calculation for input systems described in Table 3; mass of target alloy 7500 g [16]

Alloy	metal [g]	slag [g]
Al-Cr-Ti	6826.8	11771.0
Al-Ti-V	6993.5	12126.0
Al-Cr-V	7408.9	9386.8
Al-Cr-Ti-V	7035.9	12345.0
Al-Cr-Ti-V (adj.)	7081.9	15327.0
Al-Cr-Mo-Ti-V (adj.)	7127.6	11353.0

Both, the thermochemical simulation of the system and the experimental work, show that the direct synthesis of the quinary RHEA Al-Cr-Mo-Ti-V by assuming stoichiometric conversion is not possible. High Ti-oxide content in the slag results in lowered Ti content in the alloy composition obtained.

Adjustment of the quaternary and quinary input system after XRF analysis did not result in any improvement. At this point, high deviation of the analytical results by XRF and ICP-OES leads to incorrect adjustment of the input material. As shown in Table 4, especially for the elements Al and Ti differences in alloy composition were recognized. For the ternary systems, Al contents measured by XRF are on average 41 % higher than in the ICP-OES analysis. The incorrect adjustment was determined after conduction of the trials.

As the Richardson-Jeffes diagram (Figure 3) shows a much lower free enthalpy of reaction for TiO_2 reduction than for Cr_2O_3, MoO_2 or V_2O_5, already obtained Ti can act as reducing agent for these metal oxides besides Al. At this point, it should be noted, that the Richardson-Jeffes diagram applies to pure substances with an activity of 1. In alloys, however, this is not the case. This causes alloy-specific changes in the Richardson-Jeffes diagram and leads to a change in the position of the free reaction enthalpy for each reaction. The compositions obtained in the series of experiments suggest that Al and Ti are significantly affected. At the beginning of the reaction, high concentration of Al is present in the metal phase, while the concentration of the other metals only increases as a result of reduction during the course of the reaction. An increase in concentration is also accompanied by an increase in activity. Both facts, the lower free enthalpy of TiO_2-reduction and the rising activity in the alloy lead to a lower Ti content in the alloy and thus, to higher Ti-oxide content in the slag phase.

Further investigation focuses on the influence of different oxides, Cr_2O_3, V_2O_5, MoO_3 and Nb_2O_5, on TiO_2 conversion during aluminothermic reduction. A better understanding of the reduction process for a variety of oxides reduced simultaneously would allow conclusions regarding the input mixture. It is also possible to produce master alloys which are fused in a subsequent remelting process step. Vacuum induction melting is conceivable for this purpose, and possibly also other processes such as vacuum arc remelting due to high liquidus temperatures of the refractory metals contained. Recommendable would be the production of a master alloy without Ti. In the presented experimental series

alloys without Ti have shown great potential and could achieve the targeted compositions. It may also be possible to improve the direct production of RHEAs by adding slag additives. For example, it is conceivable that additional TiO_2 as slag additive leads to saturation of the slag by this oxide and thus enhances the reduction of TiO_2 to Ti. Further studies are unavoidable to investigate the alloy system considered in this paper.

References

[1] Steiner, R. (1990): A.S.f. Metals, ASM Handbook Volume 1: Properties and Selection: Irons, Steels, and High-Performance Alloys, ASM International.

[2] Steiner, R. (1990): A.S.f. Metals, ASM Handbook Volume 2: Properties and Selection: Non-ferrous Alloys and Special-Purpose Materials, ASM International.

[3] Cantor, B. (2014): Multicomponent and High Entropy Alloys, Entropy, vol. 16, no. 9, pp. 4749-4768.

[4] Gao, M. C., Yeh, J. W., Liaw, P. K., & Zhang, Y. (2016): High-entropy alloys, Springer International Publishing, ISBN: 978-3-319-27011-1.

[5] Murty, B.S.; Yeh, J.W.; Ranganathan, S.; Bhattacharjee, P.P. (2019): A brief history of alloys and the birth of high-entropy alloys, in: High-Entropy Alloys (Second Edition), Elsevier, pp. 1-12.

[6] Ranganathan, S. (2003): Alloyed pleasures: multimetallic cocktails, Current science, vol. 85, no. 5, pp. 1404-1406.

[7] Yeh, J.W. (2006): Recent progress in high entropy alloys, Annales De Chimie – Science des Materieux, vol. 31, no. 6, pp. 633-648.

[8] Yeh, J. W.; Chen, S. K.; Lin, S. J.; Gan, J. Y.; Chin, T. S.; Shun, T. T.; Chang, S. Y. (2004): Nanostructured high-entropy alloys with multiple principal elements: novel alloy design concepts and outcomes, Advanced Engineering Materials, vol. 6, no. 5, pp. 299-303.

[9] Gottstein, G. (2013): Materialwissenschaft und Werkstofftechnik: Physikalische Grundlagen, 4. Auflage , ISBN 0937-7433, Springer-Verlag.

[10] Atkins, P. W.; De Paula, J. (2013). Physikalische Chemie, 5. Auflage, ISBN 978-3-527-33247-2, John Wiley & Sons.

[11] Yeh, J. W. (2013): Alloy design strategies and future trends in high-entropy alloys, JOM, vol. 65, no. 12, pp. 1759-1771.

[12] Murty, B. S.; Yeh, J. W.; Ranganathan, S.; Bhattacharjee, P. P. (2019): High-entropy alloys, Elsevier.

[13] Zhang, Y.; Zuo, T.T.; Tang, Z.; Gao, M.C.; Dahmen, K.A.; Liaw, P.K.; Lu Z.P. (2014): Microstructures and properties of HEA, Progress in Materials Science, vol. 61, pp. 1-93.

[14] Kieffer, R.; Jangg, G.; Ettmayer, P. (1971): Metallurgie der Sondermetalle, in: Sondermetalle, pp. 27-147, Springer, Wien.

[15] Dautzenberg, W. (1974): Aluminothermie, in: Ullmanns Encyklopädie der technischen Chemie, pp. 351 - 361, Bartholome, E.; Biekert, E.; Hellmann, H.; Ley, H., Weinheim/Bergstraße.

[16] Bale, C. W.; Bélisle, E.; Chartrand, P.; Decterov, S. A.; Eriksson, G.; Gheribi, A.E.; Hack, K.; Jung, I.H.; Kang, Y.B.; Melançon, J.; Pelton, A.D.; Petersen, S.; Robelin, C.; Sangster, J.; Spencer, P. and Van Ende, M.-A. (2016): FactSage Thermochemical Software and Databases - 2010 - 2016, Calphad, vol. 54, pp. 35-53.

[17] Richardson, F. D.; Jeffes, J. H. E. (1948): The Thermodynamics of Substances of Interest in Iron and Steel Making, Part I - Oxides Journal of the Iron and Steel Institute, vol: 160, pp. 261-270 ISSN: 0021-1567.

[18] Coudurier, L.; Hopkins, D. W.; Wilkomirsky, I. (1985): Fundamentals of Metallurgical Processes, vol 2, Pergamon Press, ISBN: 978-0-08-032536-1

[19] Stoephasius, J.-C.; Friedrich, B. (2004): Modellierung metallothermischer Reaktionen - Berechnung der Einsatzmischung unter Berücksichtigung energetischer Effekte, Erzmetall - World of Metallurgy, vol. 57, no. 4, pp. 217 - 224.

[20] Udoeva, L.Y.; Chumarev, V.M.; Larionov, A.V.; Rylov, A.N.; Trubachev, M.V. (2013): Simulation of the aluminothermic smelting of Mo-Ti-Al and Mo-Ti-V-Cr-Al alloys, Russian Metallurgy (Metally), vol. 8, pp. 564-569.